




Separating chiral isomers of amphetamine and methamphetamine using chemical derivatization and differential mobility spectrometry

J. Larry Campbell^{1,2,3,5,*}  | Amol Kafle¹ | Zack Bowman^{2,4} | J. C. Yves Le Blanc¹ | Chang Liu¹ | W. Scott Hopkins^{2,4,5}

¹ SCIEX, Concord, Ontario, Canada

² Department of Chemistry, University of Waterloo, 200 University Avenue West, Waterloo, Ontario, Canada

³ Bedrock Scientific, Milton, Ontario, Canada

⁴ Waterloo Institute for Nanotechnology, University of Waterloo, 200 University Avenue West, Waterloo, Ontario, Canada

⁵ WaterMine Innovation, Inc., Waterloo, Ontario, Canada

Correspondence

J. Larry Campbell, Bedrock Scientific Inc., Milton, Ontario, Canada.

Email: larry.campbell@bedrockscientific.com
W. Scott Hopkins, Department of Chemistry, University of Waterloo, 200 University Avenue West, Waterloo, ON, Canada.
Email: scott.hopkins@uwaterloo.ca

* Current address: J. Larry Campbell, Bedrock Scientific Inc., Milton, ON, Canada.

Abstract

The separation and analysis of chiral compounds, especially enantiomers, presents a great challenge to modern analytical chemistry, particularly to mass spectrometry (MS). As a result, integrated orthogonal separations, such as chiral liquid chromatography (chiral LC), gas chromatography (GC), or capillary electrophoresis (CE), are often employed to separate enantiomers prior to MS analysis. Here, we combine chemical derivatization with differential mobility spectrometry (DMS) and MS to separate and quantify the transformed enantiomeric pairs R- and S-amphetamine, as well as R- and S-methamphetamine. We also demonstrate separation of these drugs by using reverse-phase LC. However, while the LC method requires ~5 min to provide separation, we have developed a flow-injection analysis (FIA) method using DMS as the exclusive mode of separation (FIA-DMS), requiring only ~1.5 min with equivalent quantitative metrics (1-1000 ng/mL range) to the LC method. The DMS-based separation of each diastereomeric pair is driven by differences in binding energies between the analyte ions and the chemical modifier molecules (acetonitrile) added to the DMS environment.

KEYWORDS

Chiral, differential mobility spectrometry, isomers, mass spectrometry, quantitation

1 | INTRODUCTION

While modern mass spectrometers are powerful analytical tools, their use for identifying and quantifying certain isomeric species can be limited. This is especially true of chiral isomers,¹ molecules whose mirror images are not identical nor superimposable. Most commonly, chiral isomers differ by the orientation of four different substituents bonded to a central atom, typically carbon.² Among chiral isomers, enantiomers – non-superimposable mirror image isomers – present an ongoing analytical challenge. Chiral isomers cannot be differentiated by their m/z nor by comparing only subtle differences between intensities of iden-

tical fragment ions (ie, MS/MS spectra). Even then, the MS/MS analysis of a convolved mixture of chiral isomers can be difficult to interpret. Consequently, MS analyses of chiral compounds usually rely upon some form of orthogonal separation prior to MS analysis. For brevity, this manuscript will focus on the technologies applied to one specific analytical target – amphetamines – but readers are directed to a broader and more thorough review on this subject.¹

Amphetamines are a class of stimulant drugs that can present a number of safety and legal issues.³ One of the challenges facing the bioanalysis of amphetamine-based drugs in human samples stems from the fact that amphetamine (AMP), and its closely related

This is an open access article under the terms of the [Creative Commons Attribution-NonCommercial-NoDerivs](https://creativecommons.org/licenses/by-nc-nd/4.0/) License, which permits use and distribution in any medium, provided the original work is properly cited, the use is non-commercial and no modifications or adaptations are made.

© 2020 The Authors. *Analytical Science Advances* published by Wiley-VCH GmbH

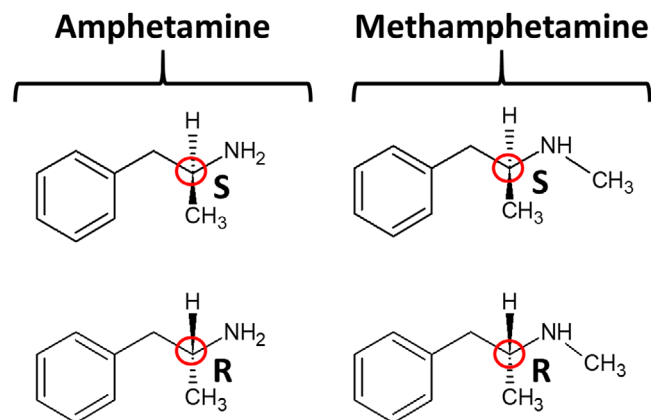


FIGURE 1 The enantiomers of amphetamine and methamphetamine

analogue, methamphetamine (MeAMP), can each exist in one of two enantiomeric forms: either the R- or S- orientation of substituents positioned around a central carbon atom (Figure 1). This designation of chirality is made following the Cahn-Ingold-Prelog convention wherein the priorities of different substituents leads the assignment.⁴ Interestingly, while both AMP and MeAMP are listed as a Schedule II controlled substances within the US Controlled Substances Act, there is no specification related to the stereochemistry of these molecules.⁵ Specifically, each drug's S-isomer is a Schedule II drug (ie, as a powerful stimulant), while the less potent R-isomers find legally permissible pharmaceutical uses (ie, R-MeAMP has been marketed as a decongestant and is a much less potent stimulant than its S-analogue).^{6,7} Persons using the S-isomers illegally could conceivably attempt to mask detection of the drug by co-dosing with the R-isomers, assuming the test for one enantiomer could be interfered with by the other. As a result, a fast and sensitive technique would be highly valuable to differentiate these enantiomeric pairs rapidly and with adequate sensitivity.

Several analytical approaches have been utilized to separate and identify the enantiomers of AMP and MeAMP. One of the earliest routine methods combined chemical derivatization and gas chromatography (GC),^{8,9} with (S)-N-trifluoroacetyl prolyl chloride (TPC) standing out as a popular reagent. TPC reacts quantitatively with AMP and MeAMP to form a structure with two chiral centers – a diastereomer. Reactions with TPC, itself a chiral molecule supplied commercially with an enantiomeric excess of $\geq 96.5\%$, ensures that one of the chiral centers (introduced by the TPC moiety) is of known chirality. Like most GC-based derivatization strategies, the new structure is less polar and more thermally stable than the analyte itself, improving GC sample handling and separation. Typically, the GC-based separation of the isomers of TPC-AMP and TPC-MeAMP, which does not require chiral stationary phases for the columns, require run times in the order of tens of minutes.^{8–11} Besides GC, liquid chromatography (LC) methods have been developed for the separation of enantiomers like AMP and MeAMP,¹¹ with popular chiral stationary phases consisting of vancomycin, a polysaccharide drug that contains 18 chiral centers,¹² and β -cyclodextrin¹³ among several others. Similar chiral stationary phases

have also been successfully employed in capillary electrophoresis (CE)-based workflows for separation of AMP and MeAMP.^{14,15}

Beyond specialized chromatographic methods, attempts to separate pairs of chiral compounds have also employed gas-phase chemistry and modern ion mobility spectrometry (IMS) methods.¹⁶ In one example, a conventional drift-time IMS experiment was augmented by the addition of volatile, chiral molecules (eg, (S)-2-butanol) to the nitrogen drift gas.¹⁷ Although the nitrogen-only environment provided no separation, the addition of the chiral dopant induced separation of enantiomeric pairs of ions. While these preliminary experiments showed some promise, other recent studies^{18,19} indicate that the “three-point interaction” model for small gas-phase ions (eg, $< m/z$ 500) and volatile chiral molecules (eg, S-(+)-2-butanol) does not hold.^{20,21} A more likely ion/molecule binding interaction would be dominated by ion-dipole interactions, which is not driven by the same weaker, more subtle chiral site interactions.²²

Differential mobility spectrometry (DMS) is another IMS technique that can separate isomeric species.^{23–48} Unlike drift-time or traveling-wave IMS, where differences in ions' collision cross sections are probed under low-electric field conditions, DMS separates ions based upon differences in their mobilities under high- and low-electric field conditions established in the DMS cell (Figure 2A,B).¹⁶ Here, ions are carried by a gas flow between two planar, parallel electrodes that bear a radio-frequency asymmetric voltage (the separation voltage or SV) that establishes the dynamic high- and low-electric field conditions.⁴⁹ As the SV is increased, ions acquire “zig-zag” trajectories of increasing widths as they traverse the DMS cell. This off-axis component to the trajectory increases non-linearly with increasing SV. Ultimately, ions require a DC compensation voltage (CV) to bring their flight paths on axis for successful sampling by a mass spectrometer.

While DMS has previously been employed to separate AMP from ambient chemical noise,⁵⁰ no examples of the separation of AMP's enantiomers have been published. A handful of methods have demonstrated the separation of chiral compounds using high-field asymmetric waveform ion mobility spectrometry (or FAIMS),⁵¹ an analogue of DMS where the electrodes are cylindrical, not planar. All of these studies rely on the formation of noncovalent ion/molecule clusters that are diastereomeric by virtue of their composition. In one iteration, diastereomeric cluster ions were formed consisting of the chiral analyte, a divalent metal ion core, and homochiral “reference” ligands (eg, L-amino acids).^{52,53} Unfortunately, each chiral analyte required a unique metal ion/reference ligand combination that, by the authors' own descriptions, did not follow any definitive, predictable trends. More recently, another group demonstrated the DMS-based separation of enantiomers (eg, amino acids) after being electrosprayed with a pure chiral binding partner (eg, N-tertbutyloxycarbonyl-O-benzyl-L-serine) without any metal ions.^{54,55} However, current detection limits of those chiral species are still not low enough for bioanalytical use (ie, hundreds of μM [or $\mu\text{g}/\text{mL}$] instead of the low ng/mL required) and ion source contamination could result from the required use of high concentrations of the cluster components.

Based on these insights from the literature, we focused our study on the use of a chemical derivatization-based approach for

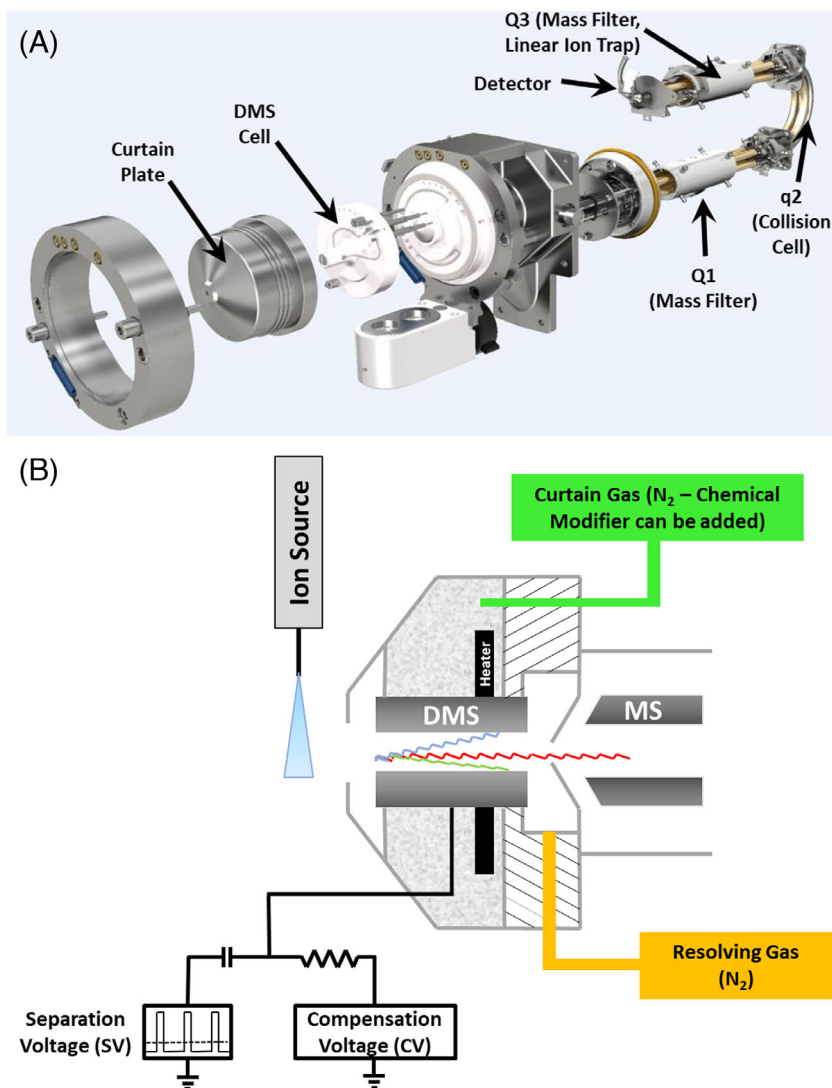


FIGURE 2 A, Schematic diagram of the DMS cell coupled to a hybrid triple quadrupole-linear ion trap MS system employed in this study. B, Between the DMS electrodes, several ions' trajectories are depicted as colored "zig zag" lines, which occurs as ions experience the electric fields established by the asymmetric RF waveform (separation voltage, SV) and dc voltage (compensation voltage, CV); only the red ions successfully transit the DMS cell

separating the enantiomers of both AMP and MeAMP by DMS. Our initial investigations explored the utility of this workflow.⁵⁶ Recently, another group followed a similar rationale by showing separation of covalently derivatized amino acid enantiomers using trapped ion mobility spectrometry.⁵⁵ We also endeavored to employ LC separation in concert, since LC provides a degree of sample desalting and purification, even when implemented in an unoptimized fashion.

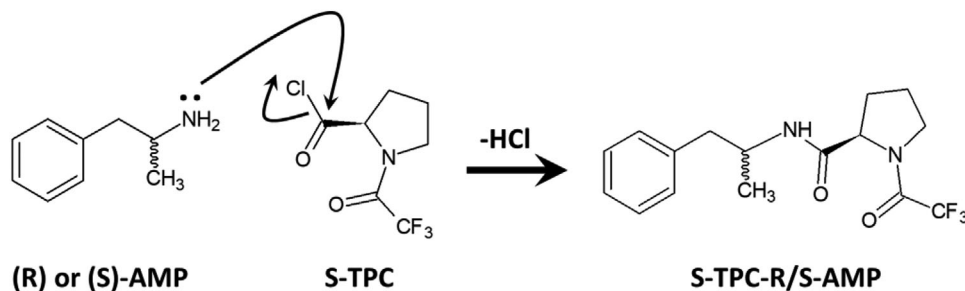
2 | EXPERIMENTAL SECTION

2.1 | Chiral compounds and their derivatization

Amphetamine (AMP) and methamphetamine (MeAMP) standards, including individual enantiomerically pure species and their racemic

mixtures were purchased from Cerilliant Corporation (Round Rock, TX). The derivatizing reagent used, (L)-N-trifluoroacetyl prolyl chloride (S-TPC) (enantiomeric excess $\geq 96.5\%$), was purchased from Sigma-Aldrich (Oakville, ON). All compounds were used as received and without further purification.

To derivatize the analytes, 12.5 μL aliquots of stock analyte solutions (1 mg/mL) were added to a 500 μL capped Eppendorf tube. The liquid was dried down using a flow of nitrogen gas, after which the solution was reconstituted by the addition of 100 μL of hexanes and 100 μL of TPC solution. After sealing the vial and vortexing (500 rpm) for 10 s, the vial was heated for 15 min at 70°C with 500 rpm of shaking. This solution was dried down and reconstituted with 250 μL of 50/50 water/acetonitrile with 0.1% formic acid. A 30 μL aliquot of sample solution was mixed with 1470 μL of 50/50 water/acetonitrile with 0.1% formic acid to make a working stock solution of 1000 ng/mL concentration. This solution was then diluted by 10x using the same



SCHEME 1 Reaction of amphetamine (AMP) with (L)-N-trifluoroacetyl prolyl chloride (S-TPC)

solvent system to provide a calibration curve sample set at 1, 10, 100, and 1000 ng/mL.

2.2 | Matrix sample preparation

Rat urine (500 μL) was used as a matrix to test the workflow. Sample clean-up was performed using a Strata-X Drug B kit (Phenomenex, Torrance, CA, USA) strong cation exchange with mixed-mode sorbent for the solid-phase extraction (SPE) procedure. First, 250 μL of 50 mM phosphate buffer (pH 6) was added to the sample before loading onto the SPE column. No equilibration of the SPE cartridges was necessary. The cartridge was then washed with 1 mL of 100 mM sodium acetate (pH 5) followed by a further wash with 1 mL methanol. The SPE cartridge was dried under full vacuum for 5 min and the analytes eluted using 500 μL of a mixture of ethyl acetate, isopropyl alcohol, and ammonium hydroxide (70:20:10). Both AMP and MeAMP samples were then spiked into 250 μL this matrix, dried down, and this mixture was subjected to the TPC derivatization reaction as shown in Scheme 1. Different amounts of AMP and MeAMP enantiomers were spiked into four matrix samples yielding samples with final analyte concentrations of 1, 10, 100, and 1000 ng/mL.

2.3 | DMS-MS/MS infusion conditions

A differential mobility spectrometer (Figure 2A) was mounted in the atmospheric region between the sampling orifice and electrospray ionization (ESI) source (5500 V) of a hybrid triple quadrupole – linear ion trap mass spectrometer (Figure 2B). The temperature of the DMS cell was maintained at $T = 150^\circ\text{C}$, and the nitrogen curtain gas was operated at 10 psi. The fundamentals of the DMS device have been described elsewhere.^{16,23,48,57–59} In this study, the separation voltage (SV) was held at $SV = 4000\text{ V}$ while the compensation voltage (CV) was scanned from $CV = -40\text{ V}$ to $+20\text{ V}$ in 0.25 V increments. DMS chemical modifier flow (acetonitrile) provided by an external Shimadzu LC10ADvp pump (connected to the communications bus module of a Shimadzu Prominence XR) was set to yield a 1.5% (mole ratio) concentration of acetonitrile in the curtain (carrier) gas flow.

After passing through the DMS cell, ions accepted into the mass spectrometer were analyzed by multiple-reaction monitoring (MRM)

using conditions listed in Table 1. Each of the diastereomers was mass filtered with the first quadrupole (Q1), fragmented by collision-induced fragmentation (CID) with N_2 in the rf-only second quadrupole (q2), and selected fragment ions filtered by the third quadrupole (Q3). To improve selectivity and detection sensitivity, we monitored two MRM fragment channels for each analyte, with designations of “_1” and “_2” in Table 1. All of the SCIEX technology, as well as the Shimadzu HPLC modules, was controlled by Analyst[®] software (version 1.6.2).

2.4 | LC-DMS-MS/MS and FIA-DMS-MS/MS conditions

For the LC-DMS-MS/MS and FIA-DMS-MS/MS experiments conducted with the TPC-derivatized AMP and MeAMP, we performed LC separation using a Shimadzu Prominence XR (Shimadzu Scientific Instruments, Columbia, MD, USA). Samples were injected onto a Kinetex C18 column (1.7 μm , 100 \AA , 100 \times 2.1 mm) (Phenomenex, Torrance, CA) held at 40°C , and analytes were eluted from the column using one of the two methods: (LC separation) 50 to 70% B in 4.0 min, to 95% B at 4.2 min, holding to 4.3 min, then returning to 50% B at 5.0 min; (FIA – no separation): Isocratic elution at 85% B (Solvent A = water + 0.1% formic acid; Solvent B = methanol + 0.1% formic acid; flow rate of 700 $\mu\text{L}/\text{min}$; injection volume of 10 μL). The optimized DMS conditions during these runs were $SV = 4000\text{ V}$, DMS cell temperature $T = 225^\circ\text{C}$, Resolving (throttle) gas pressure P_{resolv} (or DR) = 6 psi, 1.5% (mole ratio) acetonitrile chemical modifier, $SV = 4000\text{ V}$, and CV was compound-dependent (see Table 1). For all of the LC-DMS-MS/MS and FIA-DMS-MS/MS experiments, the same ion source conditions were employed: ESI voltage $V_{\text{ESI}} = 5500\text{ V}$, curtain gas pressure $P_{\text{cur}} = 10\text{ psi}$, gas 1 pressure $P_1 = 60\text{ psi}$, gas 2 pressure $P_2 = 80\text{ psi}$, source temperature $T_{\text{source}} = 500^\circ\text{C}$, and declustering potential $DP = 100\text{ V}$.

Quantitation of the LC-DMS-MS/MS and FIA-DMS-MS/MS results was performed using MultiQuant[™] software. For each analyte ion, we summed the two MRM transitions collected at each CV for each analyte,⁶⁰ and employed the following signal processing functions: Gaussian smooth width of 1.0 points; RT half window of 5.0 s. Noise percentage of 40.0%, Baseline subtraction window of 2.00 min, 2 point peak splitting factor, Regression parameter set to Area; Regression type set to quadratic; Weighting type of $1/x^2$.

**TABLE 1** MRMs employed in this study

MRM Transition	Q1	Q3	CE / eV	CV / V
TPC-S-AMP_1	329.1	166.1	35	-19.6
TPC-S-AMP_2	329.1	91.0	50	-19.6
TPC_R-AMP_1	329.1	166.1	35	-13.3
TPC_R-AMP_2	329.1	91.0	50	-13.3
TPC-R-MeAMP_1	343.2	166.1	35	-3.5
TPC-R-MeAMP_2	343.2	91.0	50	-3.5
TPC-S-MeAMP_1	343.3	166.1	35	-6.3
TPC-S-MeAMP_2	343.3	91.0	50	-6.3

2.5 | Computational methods

Neutral TPC-amphetamine and TPC-methamphetamine structures were first generated and pre-optimized at the PM7 level of theory as implemented in Gaussian 16.^{61,62} Following low-level optimization, all of the various prototropic isomers for each molecule were manually generated and assessed for relative energy by re-optimization at the B3LYP/6-31++G(d,p) level of theory.⁶³ The lowest energy species were found to be protonated at the amide carbonyl. To ensure that accurate structures were obtained, a basin hopping (BH) algorithm that interfaces with the Gaussian16 software suite was employed to search the potential energy surfaces (PESs) of R- and S-TPC-amphetamine and R- and S-TPC-methamphetamine.⁶³⁻⁶⁶ The BH algorithm modeled the derivatized structures using the AMBER force field with partial charges that were calculated at the B3LYP/6-31G++(d,p) level of theory using the CHelpG method.^{68,69} The PES was sampled ~20 000 times for each molecule by applying a random rotation of $-10^\circ \leq \theta \leq 10^\circ$ to each of the dihedral angles in each protonated structure. The BH search identified ~30 unique isomers for each compound; these candidate structures were then carried forward for subsequent geometry pre-optimization at the semi-empirical PM7 level of theory, followed by optimization at the B3LYP/6-311++G(d,p) level of theory. The DFT-optimized structures were then sorted by their electronic energies to determine the most likely species present in the probed ensemble. Normal mode analyses were conducted for the global minima and isomers within ~15 kJ/mol of the global minima for each molecule. These analyses served the dual purpose of ensuring that the geometry optimized structures were local minima (rather than transition states) on the PES and providing thermochemical corrections for the electronic energies. The global minima and isomers within $\Delta G^\circ = 15$ kJ/mol were employed in subsequent calculations to model the structures and properties of ionic clusters containing a single solvent molecule. Generation of ion-solvent cluster input geometries was guided by examining the electrostatic potentials of the bare protonated molecules to identify regions of high partial positive and partial negative charge. Upon identifying these regions of the PESs, cluster structures were manually created by introducing a single acetonitrile (ACN) molecule to each region of high partial positive or partial negative charge for each isomer within $\Delta G^\circ = 15$ kJ/mol of the bare ion global minimum. The candidate struc-

tures for the ion-solvent clusters were then geometrically optimized at the B3LYP/6-311++G(d,p) level of theory.

3 | RESULTS AND DISCUSSION

3.1 | Derivatizing AMP and MeAMP with TPC enables DMS separation of their chiral isomers

The need to augment the structures of the AMP and MeAMP analytes was evident from our initial investigations on the DMS separation of these underivatized enantiomer pairs. These experiments revealed that underivatized racemic mixtures of both AMP and MeAMP were not separated (ie, observed differences in CV values) for these enantiomers (data not shown). However, since DMS has previously been used to separate diastereomers,^{23,35} we pursued a chemical derivatization approach to generate diastereomers from the target enantiomer analytes using S-TPC^{8,9} as the reagent. Aside from these previous DMS studies, we have recently separated isomeric species using DMS that exhibited different physicochemical properties^{39,48}; since diastereomers typically exhibit different physicochemical properties from one another,⁷⁰⁻⁷¹ we hypothesized that DMS separation of the TPC-AMP synthesized diastereomers should be achievable.

The TPC-derivatized forms of R- and S-AMP, as well as R- and S-MeAMP were found to be separable by DMS. When using a nitrogen-only environment for the DMS cell ($SV = 4000$ V), the separation of the TPC-MeAMP diastereomers required the use of resolving gas at a pressure of 10 psi (Figure 3A). While the use of resolving gas causes some signal reduction, it acts to provide higher resolution DMS separations to isolate isomeric species that exhibit similar CV values. To avoid the dilution of signal intensity associated with the use of resolving gas, we also wished to investigate the use of chemical modifiers added to the DMS cell via the mass spectrometer's curtain gas flow. This workflow can also provide a route to separate the ions based upon differences between how each ion binds to solvent molecules in the DMS environment.^{38,39}

The addition of acetonitrile as the modifier gas in the DMS cell resulted in negative CV shifts for each of the TPC-AMP and TPC-MeAMP diastereomers (Figure 3B). The identities of the individual

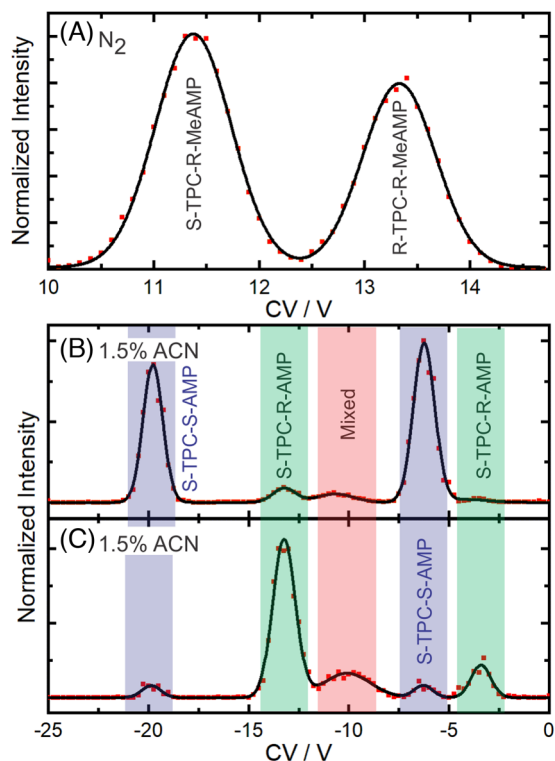


FIGURE 3 A, Separation of TPC-derivatized R- and S-MeAMP by DMS ($SV = 4000$ V) in pure nitrogen using a $DR = 10$ psi. B, Analogous experiments where 1.5% (mole ratio) acetonitrile ($SV = 4000$ V) was used to separate the S-TPC-derivatized S-isomers of AMP and MeAMP. C, Similar analyses of only the derivatized R-isomers of AMP and MeAMP. The key analyte signals and their relevant CV values are labeled (S,S- isomers highlighted in blue; S,R-isomers highlighted in green), including signal due to the presence of a cluster of S-TPC-R/S-MeAMP that transmits through the DMS at CV ~ -11 to -9.5 V (highlighted in pink). These data were acquired during low-flow (~ 15 $\mu\text{L}/\text{min}$) infusion experiments, as the CV values are slightly different compared to the LC-DMS results

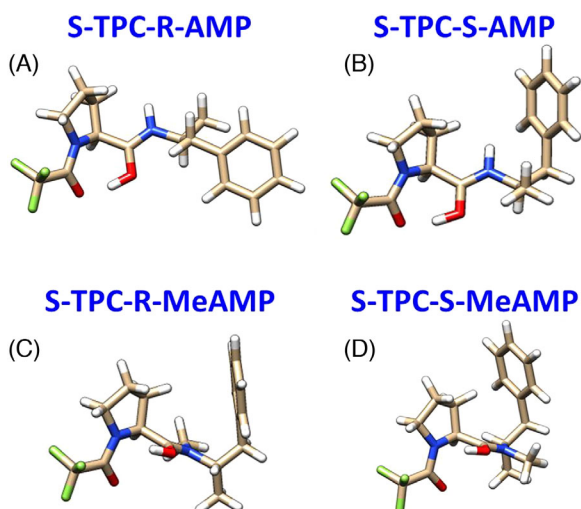


FIGURE 4 Global minimum structures of protonated A, S-TPC-R-AMP, B, S-TPC-S-AMP, C, S-TPC-R-MeAMP, and D, S-TPC-S-MeAMP as calculated at the B3LYP/6-311++G(d,p) level of theory

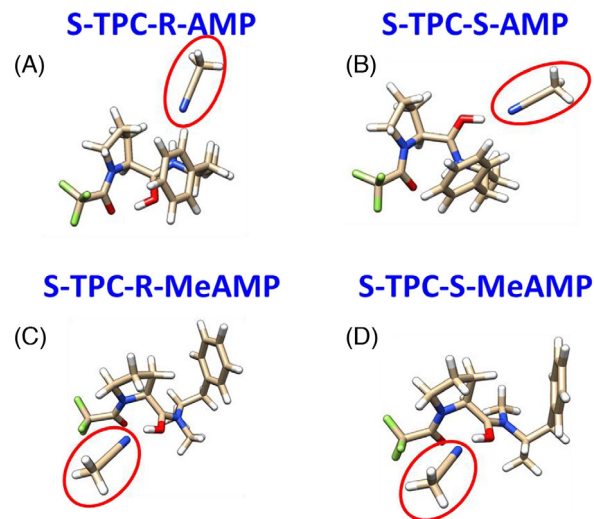


FIGURE 5 Global minimum structures of protonated A, S-TPC-R-MeAMP, B, S-TPC-S-MeAMP, C, S-TPC-R-AMP, and D, S-TPC-S-AMP each clustered to a single ACN molecule (circled in red to highlight)

diastereomers were verified by analyzing individual enantiomers of (S)- and (R)-AMP derivatized with TPC (-19.6 V for S-TPC-S-AMP, -13.3 V for S-TPC-R-AMP). Interestingly, the DMS analysis of the TPC-MeAMP diastereomers yielded three peaks in their ionograms (-9.5 , -6.3 , and -3.5 V); again, through the analysis of the individual derivatized (R)- and (S)-MeAMP, we observed that two peaks (-9.5 and -6.3 V) were attributed to S-TPC-S-MeAMP, while S-TPC-R-MeAMP also yielded two peaks (-9.5 and -3.5 V; Figure 3B). Given that the two diastereomers both produced a small peak at CV ~ -9.5 V, we attributed this signal to another form of the TPC-MeAMP ion, possibly an ion/solvent cluster. While we did record MRM signals at this CV as well, ultimately, a lack of predictable response relative to concentration changes eliminated it as an analytical target.

In all, these data confirm the identities of the peaks originating from S-TPC-S-MeAMP and S-TPC-R-MeAMP, and demonstrates how DMS can be used to separate the potential interference of isobaric chemical interferences (ie, compounds present in the mixture that yield precursor and fragment ions of the same integer m/z value).

3.2 | Computations support the DMS separation of chiral isomers

Computational modeling supports our DMS experimental findings. The derivatized S-TPC-R-AMP exhibited three isomers within $\Delta G = 15$ kJ/mol of the global minimum structure, whereas the derivatized S-TPC-S-AMP, S-TPC-R-MeAMP, and S-TPC-S-AMP species exhibited four, two, and four isomers, respectively. The lowest-energy structures of the protonated AMP and MeAMP derivatives are shown in Figure 4. For the AMP derivatives, the charge-carrying proton is shared between the carbonyl groups, while the MeAMP derivatives exhibit an O-H \cdots N H-bonding motif in the ground state.

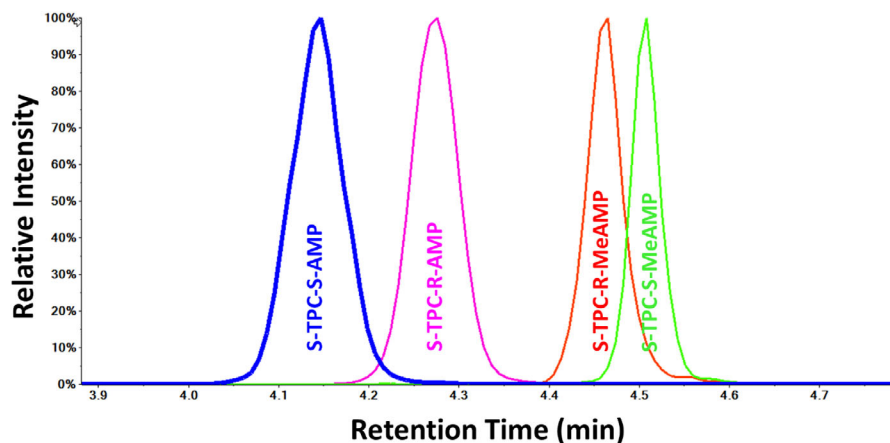


FIGURE 6 Extracted LC ion chromatograms for S-TPC-S-AMP (blue), S-TPC-R-AMP (pink), S-TPC-S-MeAMP (green), and S-TPC-R-MeAMP (red). Samples were injected from 100 ng/mL solutions prepared in 50/50 water/acetonitrile + 0.1% formic acid

Figure 5 shows the lowest-energy calculated [TPC-(Me)AMP + ACN + H]⁺ clusters; (A) S-TPC-R-AMP and (B) S-TPC-S-AMP have solvent binding energies of 31.1 and 33.1 kJ/mol, respectively, while (C) S-TPC-R-MeAMP and (D) S-TPC-S-MeAMP exhibited solvent binding energies of 33.8 and 34.8 kJ/mol, respectively. For the TPC-MeAMP species, the ACN molecule is interacting with the charge-carrying proton in an O-H...N H-bonding motif. However, for the TPC-AMP diastereomers, there was a small difference between the isomers; S-TPC-R-AMP exhibits an N-H...N motif (similar to the MeAMP derivatives) while S-TPC-S-AMP exhibits an O-H...N motif. These differences in preferred geometry stem from a balance struck between the stabilization energy of the intramolecular hydrogen bond in the AMP derivatives and destabilization of the intermolecular hydrogen bond to ACN owing to the steric hinderance created by the methyl and phenyl groups. Overall, we find that the (S,S)- diastereomers interact more strongly with ACN than do the (R,S)-diastereomers, which is consistent with the fact that the (S,S)-derivatives are more strongly Type A⁵¹ (ie, shifted to more negative CV) than are the (R,S) species. These observed trends align with first-principles-based modeling⁷² that suggests that more strongly bound ion/solvent clusters will retain larger mean cluster sizes with increasing field strengths, resulting in more negative CV shifts (ie, stronger Type-A behavior).

3.3 | Derivatized TPC-isomers of AMP and MeAMP can be separated by reversed-phase LC

In addition to the DMS-based separations, we also investigated the use of conventional reversed-phase LC (eg, C18 stationary phase, as opposed to a chiral stationary phase, such as vancomycin)^{10,12} to separate the TPC-derivatives of AMP and MeAMP. This investigation was supported by a previous study's success in resolving the AMP and MeAMP diastereomers formed after derivatization using an analogue of TPC, (S)-N-heptafluorobutyl)-prolyl chloride.⁷³ After optimization of LC flow rate, gradients, and ion source conditions (please refer to

Experimental section), we obtained separation of the four diastereomers (Figure 6).

These results were obtained using a gradient and an analytical runtime that were deemed reasonable for general laboratory use (ie, ~5 min). However, one can observe that the separation of the TPC-AMP isomers is better than that for the TPC-MeAMP isomers. Instead of extending the analytical run time to improve this separation, we decided to apply DMS to this workflow to provide an orthogonal form of separation.

3.4 | DMS minimizes reliance on LC separation of TPC-derivatized AMP and MeAMP

One of the benefits of DMS technology in quantitative analyses is the reduction of chemical noise in MRM signal channels, usually due to isobaric (but chemically distinct) chemical noise.²³ We observed this benefit in this workflow, as well, as the LC-DMS-MS/MS yields an increase in the overall signal-to-noise ratio in the analyses of TPC-derivatized amphetamine from rat urine matrix. As depicted in Figure 7, when DMS was added to the LC-MRM analysis of TPC-derivatized R- and S-amphetamine, two facets of the analytical signals became much simpler. First, the LC-DMS-MRM workflow yields much lower noise levels in the S-TPC-S-AMP MRM channel (Figure 7A). As with many DMS-based assays, while there may be a perceived drop in absolute signal compared to non-DMS assays, it is the improvement in signal-to-noise that demonstrates the true benefit of implementing this technology. The second advantage realized by using DMS in this workflow is the fact that, even though both S-TPC-R-AMP and S-TPC-S-AMP were injected into the LC, only one peak resulting from S-TPC-S-AMP was detected in the LC-DMS-MRM channel for that analyte (as established by implementing the SV/CV pairing unique to that diastereomer; Figure 7). Without DMS, two MRM channels were active for the S-TPC-S-AMP MRM channel, which is indistinguishable from its diastereomeric analogue, save the later LC retention time (Figure 7B). However, it is important to note the slight shift in that LC retention time between

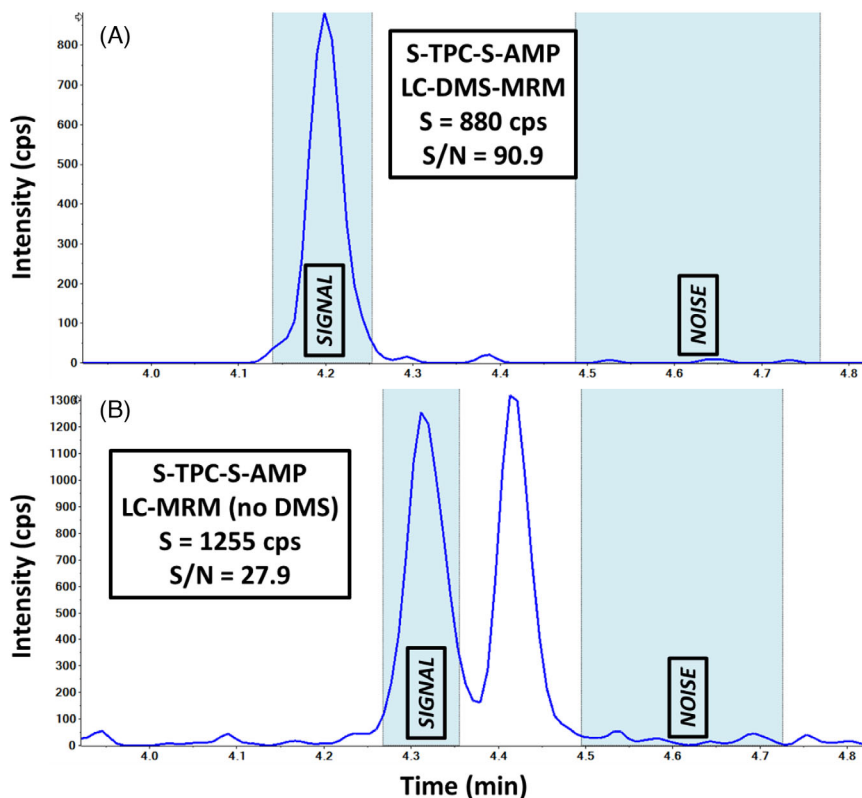


FIGURE 7 Demonstration of the impact that implementing DMS has on the LC-based analysis of S-TPC-S-AMP. When DMS is implemented A, while the overall signal is lower than without DMS present B, the signal to noise ratio (S/N) (from DMS-depleted chemical noise signals) and the simplicity of the extracted ion chromatogram (only one peak present) are evident

LC-DMS-MRM and LC-MRM experiments; such small shifts are not unheard of or unexpected, but the DMS compensates for any cross-talk resulting from such shifting in LC retention times.

Another advantage that DMS can bring to an LC-based analytical workflow is the ability to truncate the gradient length and/or amount of sample preparation needed to achieve the desired limits of quantitation (LOQs) for a given assay.⁷⁴ As noted in the discussion of the LC-only separation of the TPC-derivatized AMP and MeAMP samples (vide supra), the improvement in the chromatographic separations would require lengthening of the LC gradients or additional development time (eg, stationary or mobile phase investigation, etc). By implementing the DMS, which we had already demonstrated as being capable of separating the diastereomeric pairs of ions from each other, we can leave the chromatography as it is, or even shorten our gradient further, letting the DMS bear some of the burden of the analytical separation of these species.

We monitored the LC and DMS separations operating in concert and observed that the quality of the individual technique's separations was preserved (Figure 8). In translating the DMS parameters from the lower-flow rate infusion of standards to the LC-based introduction, we observed slight shifts in the optimal CVs for transmission of each diastereomer. These were expected as the ion source conditions (temperature, gas flows, etc) were significantly increased to support the LC and FIA conditions (ie, compared to the lower-flow infusion experiments).⁷⁵

As demonstrated in Figure 9, the simplification of the DMS-enabled detection of the derivatized amphetamines and methamphetamines to a flow-injection analysis (FIA) mode of operation was successful. Like the LC-DMS results (Figure 8), the quality of the FIA-DMS separation was evaluated by observing minimal cross-talk of MRM signals for each of the diastereomers. For example, only minute MRM signals from the S-TPC-R-AMP ions were detected in the S-TPC-S-AMP MRM channels during the LC elution time for the S-TPC-R-AMP species (Figure 8). This performance was mirrored in the results of the other diastereomers as well, and in the FIA-DMS experiments (Figure 9).

3.5 | LC-DMS and FIA-DMS provide equivalent quantitation of TPC-AMP and TPC-MeAMP isomers

The minor amount of crosstalk in the DMS-MRM channels (see Figures 8 and 9) suggested that the quantitation of these derivatized amphetamines and methamphetamines could be performed using either the LC-DMS-MS/MS or FIA-DMS-MS/MS workflows. To test this hypothesis, we assessed the quantitative statistics for the detection of the four diastereomeric drug derivatives from rat urine as determined using both methods (Table 2). Both workflows provided quality LOQs and linear dynamic ranges suitable for these analyses. Thus, if identification of both stereoisomers is required and a short (~1.5 min) analytical runtime is desired, bioanalytical results

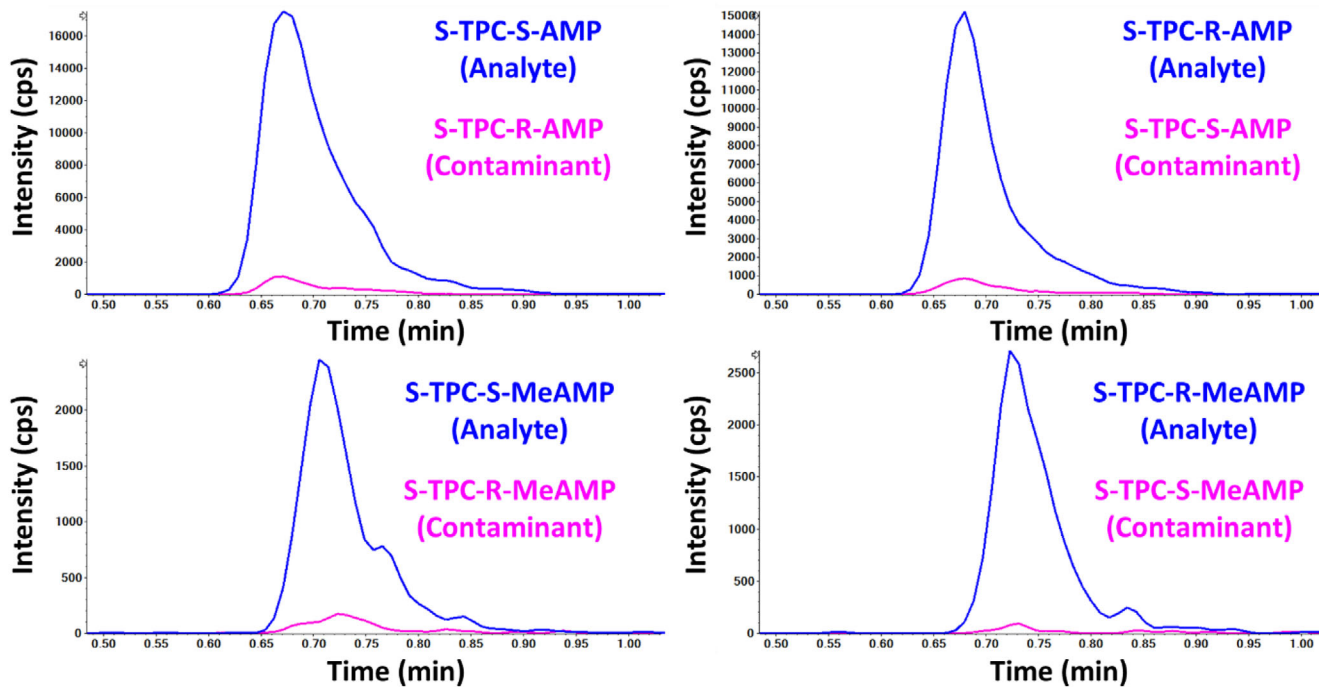


FIGURE 8 Evaluation of crosstalk in the MRM channels for each of the four diastereomers analyzed using the LC-DMS-MS/MS workflow. In each pane, the target analyte MRM signal (blue) is compared to the signal for its matching diastereomeric analogue (pink). Coincidental MRM signals are an indication of crosstalk in the analytical signal channel. In all four cases, cross-talk is 5-6%. Some retention time shifting occurred when the rat-urine matrix samples were analyzed, resulting in all analytes eluting at slightly later retention times (see text for details). Sample concentrations were 100 ng/mL in rat-urine extracted solutions

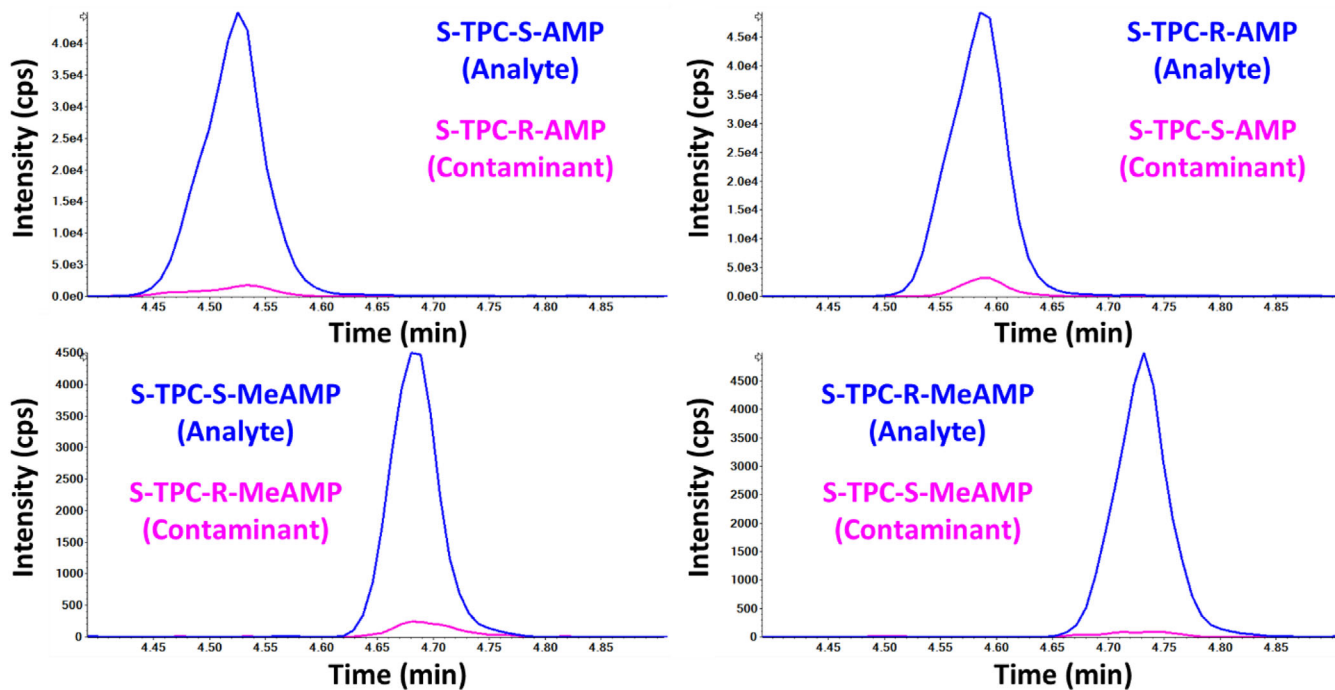


FIGURE 9 Evaluation of crosstalk in the MRM channels for each of the four diastereomers analyzed using the FIA-DMS-MS/MS workflow. In each pane, the target analyte MRM signal (blue) is compared to the signal for its matching diastereomeric analogue (pink), and coincidental MRM signals are an indication of crosstalk in the analytical signal channel. Samples were injected from 100 ng/mL solutions prepared in 50/50 water/acetonitrile + 0.1% formic acid. In all four cases, cross-talk is 5-6%

**TABLE 2** Quantitation results from both the LC-DMS-MS/MS and FIA-DMS-MS/MS calibration curves

Analyte	Actual Concentration (ng/mL)	LC-DMS-MS/MS		FIA-DMS-MS/MS	
		Accuracy (%)	Relative Standard Deviation (%)	Accuracy (%)	Relative Standard Deviation (%)
S-TPC-S-AMP	1	102.6	8.2	100.5	10.8
	10	90.2	6.6	94.7	4.9
	100	108.6	10.4	105.2	9.5
	1000	99.3	12.8	99.6	4.4
S-TPC-R-AMP	1	100.8	6.7	100.2	17.4
	10	90.7	4.0	97.7	9.1
	100	108.2	2.9	102.3	7.9
	1000	99.7	0.2	99.8	6.0
S-TPC-S-MeAMP	1	100.7	1.9	100.3	14.6
	10	92.7	16.4	96.2	8.4
	100	106.9	3.1	103.8	6.8
	1000	99.5	5.5	99.7	4.0
S-TPC-R-MeAMP	1	100.5	4.8	100.4	17.2
	10	94.0	1.8	95.8	5.9
	100	105.6	7.0	104.3	7.3
	1000	99.6	8.1	99.6	11.5

of appropriate quality are available via an FIA workflow. By analogy, an open port probe (OPP) workflow^{40,76,77} could also serve as a viable sample inlet for these DMS analyses. While the sample preparation presently requires multiple steps, this could be optimized further (eg, the extraction and derivatization steps could be combined) or samples could be batch-processed ahead of the FIA-DMS-MS/MS analyses.

4 | CONCLUSIONS

The separation and analysis of chiral compounds, especially enantiomers, presents a great challenge to modern analytical chemistry and, specifically, to MS. Distinguishing between isomers that differ only by the orientation of functional groups around a single chiral center can rarely be performed through simple tandem MS (MS/MS) experiments. Here, we applied a chemical derivatization strategy to separate the enantiomeric pairs R- and S-amphetamine and R- and S-methamphetamine using DMS. Upon derivatization of AMP and MeAMP with (L)-N-trifluoroacetyl prolyl chloride (S-TPC), not only can the enantiomeric pairs be separated using DMS, but also with reverse-phase LC. However, while the LC method requires ~5 min to provide separation, a flow-injection (higher-throughput) analysis method using DMS as the exclusive mode of separation (FIA-DMS) requires ~1.5 min, with both workflows providing equivalent quantitative metrics. The DMS-based separation of each diastereomeric pair is driven by differences in binding energies between the analyte ions and the chemical modifier molecules (acetonitrile) added to the DMS environment.

ACKNOWLEDGMENTS

WSH acknowledges NSERC funding in the form of a Discovery Grant and a Collaborative Research and Development grant, as well as support from Compute Canada.

CONFLICT OF INTEREST

The authors confirm that, at the time of writing this paper, J. Larry Campbell, Amol Kalfe, Chang Liu, and Yves LeBlanc were employed by SCIEX, a manufacturer and developer of differential mobility spectrometry and mass spectrometry technology featured in this manuscript.

DATA AVAILABILITY STATEMENT

Data presented in this manuscript can be made available upon request.

ORCID

J. Larry Campbell  <https://orcid.org/0000-0002-4496-7171>

REFERENCES

1. Awad H, El-Anead A. Enantioselectivity of mass spectrometry: challenges and promises. *Mass Spectrom Rev.* 2013;32:466-483.
2. Wu L, Vogt FG. A review of recent advances in mass spectrometric methods for gas-phase chiral analysis of pharmaceutical and biological compounds. *J Pharm Biomed Anal.* 2012;69:133-147.
3. Logan BK. Amphetamines: an update on forensic issues. *J Anal Toxicol.* 2001;25:400-404.
4. Cahn RS, Ingold CK, Prelog V. The specification of asymmetric configuration in organic chemistry. *Experientia.* 1956;12:81-94.



- Food and Drugs. *Schedules of controlled substances*, Section 812, Title 21, Ch.13, 2018; <https://www.govinfo.gov/app/details/USCODE-2017-title21/USCODE-2017-title21-chap13-subchapl-partB-sec812/summary>. Accessed November 25, 2018
- PDR Staff. *Physician's Desk Reference*. 71st ed. Montvale, NJ: Medical Economics Co; 2017.
- Logan BK. Methamphetamine - effects on human performance and behavior. *Forensic Sci Rev*. 2002;14:134-151.
- Liu JH, Ku WW. Determination of enantiomeric N-trifluoroacetyl-L-propryl chloride amphetamine derivatives by capillary gas chromatography/mass spectrometry with chiral and achiral stationary phases. *Anal Chem*. 1981;53:2180-2184.
- Fitzgerald RL, Ramos JM, Bogema SC, Poklis A. Resolution of methamphetamine stereoisomers in urine drug testing: urinary excretion of R(-)-methamphetamine following use of nasal inhalers. *J Anal Toxicol*. 1988;12:255-259.
- Wang S-M, Wang T-C, Giang Y-S. Simultaneous determination of amphetamine and methamphetamine enantiomers in urine by simultaneous liquid-liquid extraction and diastereomeric derivatization followed by gas chromatographic-isotope dilution mass spectrometry. *J Chromatogr B*. 2005;816:131-143.
- Plotka JM, Biziuk M, Morrison C. Common methods for the chiral determination of amphetamine and related compounds I. Gas, liquid and thin-layer chromatography. *Trends Anal Chem*. 2011;30:1139-1158.
- Wang T, Shen B, Shi Y, Xiang P, Yu Z. Chiral separation and determination of R/S-methamphetamine and its metabolite R/S-amphetamine in urine using LC-MS/MS. *Forensic Sci Int*. 2015;246:72-78.
- Herráez-Hernández R, Campriñs-Falcó P, Verdú-Andrés J. Strategies for the enantiomeric determination of amphetamine and related compounds by liquid chromatography. *J Biochem Biophys Meth*. 2002;54:147-167.
- Cherkaoui S, Rudaz S, Varesio E, Veuthey J-L. On-line capillary electrophoresis-electrospray mass spectrometry for the stereoselective analysis of drugs and metabolites. *Electrophoresis*. 2001;22:3308-3315.
- Shamsi SA. Chiral capillary electrophoresis-mass spectrometry: modes and applications. *Electrophoresis*. 2002;23:4036-4051.
- Eiceman G, Karpas Z, Hill HH, Jr. *Ion Mobility Spectrometry*. 3rd ed. Boca Raton, FL: CRC Press; 2013.
- Dwivedi P, Wu C, Matz LM, Clowers BH, Siems WF, Hill HH. Gas-Phase chiral separations by ion mobility spectrometry. *Anal Chem*. 2006;78:8200-8206.
- Holness HK, Jamal A, Mebel A, Almirall JR. Separation mechanism of chiral impurities, ephedrine and pseudoephedrine, found in amphetamine-type substances using achiral modifiers in the gas phase. *Anal Bioanal Chem*. 2012;404:2407-2416.
- Kulyk K, Rebrov O, Ryding M, Thomas R, Uggerud E, Larsson M. *J Am Soc Mass Spectrom*. 2017;28:2686-2691.
- Ahn S, Ramirez J, Grigorean G, Lebrilla CB. Chiral recognition in gas-phase cyclodextrin: amino acid complexes—Is the three point interaction still valid in the gas phase? *J Am Soc Mass Spectrom*. 2001;12:278-287.
- Berthod A. Chiral recognition mechanisms. *Anal Chem*. 2006;78:2093-2099.
- Nachtigall FM, Rojas M, Santos LS. MALDI coupled to modified traveling wave ion mobility mass spectrometry for fast enantiomeric determination. *J Mass Spectrom*. 2018;53:693-699.
- Schneider BB, Covey TR, Coy SL, Krylov EV, Nazarov EG. Planar differential mobility spectrometer as a pre-filter for atmospheric pressure ionization mass spectrometry. *Int J Mass Spectrom*. 2010;298:45-54.
- Shvartsburg AA, Creese AJ, Smith RD, Cooper HJ. Separation of peptide isomers with variant modified sites by high-resolution differential ion mobility spectrometry. *Anal Chem*. 2010;82:8327-8334.
- Campbell JL, Le Blanc JCY, Schneider BB. Probing electrospray ionization dynamics using differential mobility spectrometry: the curious case of 4-aminobenzoic acid. *Anal Chem*. 2012;84:7857-7864.
- Campbell JL, Zhu M, Hopkins WS. Ion-molecule clustering in differential mobility spectrometry: lessons learned from tetraalkylammonium cations and their isomers. *J Am Soc Mass Spectrom*. 2014;25:1583-1591.
- Campbell JL, Yang AM-Ci, Melo LR, Hopkins WS. Studying gas-phase interconversion of tautomers using differential mobility spectrometry. *J Am Soc Mass Spectrom*. 2016;27:1277-1284.
- Campbell JL, Baba T, Liu C, Lane CS, Le Blanc JCY, Hager JW. Analyzing glycopeptide isomers by combining differential mobility spectrometry with electron- and collision-based tandem mass spectrometry. *J Am Soc Mass Spectrom*. 2017;28:1374-1381.
- Creese AJ, Cooper HJ. Separation and identification of isomeric glycopeptides by high field asymmetric waveform ion mobility spectrometry. *Anal Chem*. 2012;84:2597-2601.
- Creese AJ, Cooper HJ. Separation of cis and trans isomers of polyproline by faims mass spectrometry. *J Am Soc Mass Spectrom*. 2016;27:2071-2074.
- Maccarone AT, Duldig J, Mitchell TW, Blanksby SJ, Duchoslav E, Campbell JL. Characterization of acyl chain position in unsaturated phosphatidylcholines using differential mobility-mass spectrometry. *J Lipid Res*. 2014;55:1668-1677.
- Noestheden MR, Headley JV, Peru KM, et al. Rapid characterization of naphthenic acids using differential mobility spectrometry and mass spectrometry. *Environ Sci Technol*. 2014;48:10264-10272.
- Beach DG, Melanson JE, Purves RW. Analysis of paralytic shellfish toxins using high-field asymmetric waveform ion mobility spectrometry with liquid chromatography-mass spectrometry. *Anal Bioanal Chem*. 2015;407:2473-2484.
- Beach DG, Kerrin ES, Quilliam MA. Selective quantitation of the neurotoxin BMAA by use of hydrophilic-interaction liquid chromatography-differential mobility spectrometry-tandem mass spectrometry (HILIC-DMS-MS/MS). *Anal Bioanal Chem*. 2015;407:8397-8409.
- Jónasdóttir HS, Papan C, Fabritz S, et al. Differential mobility separation of leukotrienes and protectins. *Anal Chem*. 2015;87:5036-5040.
- Kaszycki JL, Bowman AP, Shvartsburg AA. Ion mobility separation of peptide isotopomers. *J Am Soc Mass Spectrom*. 2016;27:795-799.
- Bowman AP, Abzalimov RR, Shvartsburg AA. Broad separation of isomeric lipids by high-resolution differential ion mobility spectrometry with tandem mass spectrometry. *J Am Soc Mass Spectrom*. 2017;28:1552-1561.
- Liu C, Le Blanc JCY, Shields J, et al. Using differential mobility spectrometry to measure ion solvation: an examination of the roles of solvents and ionic structures in separating quinoline-based drugs. *Analyst*. 2015;140:6897-6903.
- Liu C, Le Blanc JCY, Schneider BB, et al. Assessing physicochemical properties of drug molecules via microsolvation measurements with differential mobility spectrometry. *ACS Central Sci*. 2017;3:101-109.
- Liu C, Gómez-Ríos GA, Schneider BB, et al. Fast quantitation of opioid isomers in human plasma by differential mobility spectrometry/mass spectrometry via SPME/open-port probe sampling interface. *Anal Chim Acta*. 2017;991:89-94.
- Manicke NE, Belford M. Separation of opiate isomers using electrospray ionization and paper spray coupled to high-field asymmetric waveform ion mobility spectrometry. *J Am Soc Mass Spectrom*. 2015;26:701-705.
- Rorrer LC, Yost RA. Solvent vapor effects in planar high-field asymmetric waveform ion mobility spectrometry: solvent trends and temperature effects. *Int J Mass Spectrom*. 2015;378:336-346.
- Šála M, Lisa M, Campbell JL, Holčapek M. Determination of triacylglycerol regioisomers using differential mobility spectrometry. *Rapid Commun Mass Spectrom*. 2016;30:256-264.



44. Willems JL, Khamis MM, Mohammed Saeid W, et al. Analysis of a series of chlorogenic acid isomers using differential ion mobility and tandem mass spectrometry. *Anal Chim Acta*. 2016;933:164-174.
45. Berthias F, Maatoug B, Glish GL, Moussa F, Maitre P. Resolution and assignment of differential ion mobility spectra of sarcosine and isomers. *Am Soc Mass Spectrom*. 2018;29:752-760.
46. Poad BLJ, Maccarone AT, Yu H, et al. Differential-Mobility spectrometry of 1-deoxysphingosine isomers: new insights into the gas phase structures of ionized lipids. *Anal Chem*. 2018;90:5343-5351.
47. Psutka JM, Dion-Fortier A, Dieckmann T, Campbell JL, Segura PA, Hopkins WS. Identifying fenton-reacted trimethoprim transformation products using differential mobility spectrometry. *Anal Chem*. 2018;90:5352-5357.
48. Walker SWC, Anwar A, Psutka JM, et al. Determining molecular properties with differential mobility spectrometry and machine learning. *Nat Commun*. 2018;9:5096.
49. Krylov EV, Nazarov EG, Miller RA. Differential mobility spectrometer: model of operation. *Int J Mass Spectrom*. 2007;266:76-85.
50. Ayodeji I, Vazquez T, Bailey R, Evans-Nguyen T. Rapid pre-filtering of amphetamine and derivatives by direct analysis in real time (DART)-differential mobility spectrometry (DMS). *Anal Methods*. 2017;9:5044-5051.
51. Purves RW, Guevremont R. Electrospray ionization high-field asymmetric waveform ion mobility spectrometry-mass spectrometry. *Anal Chem*. 1999;71:2346-2357.
52. Mie A, Jörentén-Karlsson M, Axelsson B-O, Ray A, Reimann CT. Enantiomer separation of amino acids by complexation with chiral reference compounds and high-field asymmetric waveform ion mobility spectrometry: preliminary results and possible limitations. *Anal Chem*. 2007;79:2850-2858.
53. Mie A, Ray A, Axelsson B-O, Jörentén-Karlsson M, Reimann CT. Terbutaline enantiomer separation and quantification by complexation and field asymmetric ion mobility spectrometry-tandem mass spectrometry. *Anal Chem*. 2008;80:4133-4140.
54. Zhang JD, Mohibul Kabir KM, Lee HE, Donald WA. Chiral recognition of amino acid enantiomers using high-definition differential ion mobility mass spectrometry. *Int J Mass Spectrom*. 2018;428:1-7.
55. Zhang JD, Kabir KMM, Donald WA. Metal-ion free chiral analysis of amino acids as small as proline using high-definition differential ion mobility mass spectrometry. *Anal Chim Acta*. 2018;1036:172-178.
56. Campbell JL, Liu C, Le Blanc JCY. Using differential mobility spectrometry to study chiral compounds. Proceedings of the 21st International Mass Spectrometry Conference, Toronto, ON, Canada; August 20-26, 2016.
57. Pérez-Míguez R, Bruyneel B, Castro-Puyana M, Marina ML, Somsen GW, Domínguez-Vega E. Chiral discrimination of DL-Amino acids by trapped ion mobility spectrometry after derivatization with (+)-1-(9-Fluorenyl)ethyl chloroformate. *Anal Chem*. 2019;91:3277-3285.
58. Shvartsburg AA. *Differential Ion Mobility: Non-Linear Ion Transport and Fundamentals of FAIMS*. Boca Raton, FL: CRC Group, Taylor and Francis LLC; 2008.
59. Schneider BB, Nazarov EG, Londry F, Vouros P, Covey TR. Differential mobility spectrometry/mass spectrometry history, theory, design optimization, simulations, and applications. *Mass Spectrom Rev*. 2016;35:687-737.
60. Anderson L, Hunter CL. Quantitative mass spectrometric multiple reaction monitoring assays for major plasma proteins. *Mol Cell Proteom*. 2006;5:573-588.
61. a) Frisch MJ, Trucks GW, Schlegel HB, et al., *Gaussian 09, Revision A.02*. Wallingford, CT: Gaussian, Inc.; 2009; b) Stewart JJP. Optimization of parameters for semiempirical methods VI: more modifications to the NDDO approximations and re-optimization of parameters. *J Molecular Mod*. 2013;19:1-32.
62. Řezáč J, Fanfrlík J, Salahub D, Hobza P. Semiempirical quantum chemical PM6 method augmented by dispersion and H-Bonding correction terms reliably describes various types of noncovalent complexes. *J Chem Theory Comput*. 2009;5:1749-1760.
63. Becke AD. Density-functional exchange-energy approximation with correct asymptotic behavior. *Phys Rev A: At, Mol, Opt Phys*. 1988;38:3098.
64. Fu W, Xiong J, Lecours MJ, et al. The structures of proton-bound dimers of glycine with phenylalanine and pentafluorophenylalanine. *J Mol Spectrosc*. 2016;330:194-199.
65. Fu W, Hopkins WS. Applying machine learning to vibrational spectroscopy. *J Phys Chem A*. 2018;122:167-171.
66. Hopkins WS, Marta RA, McMahon TB. Proton-Bound 3-Cyanophenylalanine trimethylamine clusters: isomer-specific fragmentation pathways and evidence of gas-phase zwitterions. *J Phys Chem A*. 2013;117:10714-10718.
67. Lecours MJ, Chow WCT, Hopkins WS. Density functional theory study of $Rh_n S^{0\pm}$ and $Rh_{n+1}^{0\pm}$ ($n = 1-9$). *J Phys Chem A*. 2014;118:4278-4287.
68. Wiberg KB, Rablen PR. Comparison of atomic charges derived via different procedures. *J Comput Chem*. 1993;14:1504.
69. Pearlman DA, Case DA, Caldwell JW, et al. AMBER, a package of computer programs for applying molecular mechanics, normal mode analysis, molecular dynamics and free energy calculations to simulate the structural and energetic properties of molecules. *Comp Phys Commun*. 1995;91:1-41.
70. Toyo'oka T. Resolution of chiral drugs by liquid chromatography based upon diastereomer formation with chiral derivatization reagents. *J Biochem Biophys Methods*. 2002;54:25-56.
71. Hutt AJ. Drug chirality and its pharmacological consequences. In: Smith HJ, ed. *Smith and Williams' Introduction to the Principles of Drug Design and Action*. Boca Raton, FL: Taylor and Francis LLC; 2006:117-183.
72. Haack A, Crouse J, Schlüter F-J, Benter T, Hopkins WS. A first principle model of differential ion mobility: the effect of ion-solvent clustering. *J Am Soc Mass Spectrom*. 2019;30:2711-2725.
73. Leis HJ, Fauler G, Windischhofer W. Enantioselective quantitative analysis of amphetamine in human plasma by liquid chromatography/high-resolution mass spectrometry. *Anal Bioanal Chem*. 2014;406:4473-4480.
74. Ray JA, Kushnir MM, Yost RA, Rockwood AL, Wayne Meikle A. Performance enhancement in the measurement of 5 endogenous steroids by LC-MS/MS combined with differential ion mobility spectrometry. *Clin Chim Acta*. 2015;438:330-336.
75. Schneider BB, Covey TR, Coy SL, Krylov EV, Nazarov EG. Control of chemical effects in the separation process of a differential mobility mass spectrometer system. *Eur J Mass Spectrom*. 2010;16:57-71.
76. Van Berkel GJ, Kertesz V. An open port sampling interface for liquid introduction atmospheric pressure ionization mass spectrometry. *Rapid Commun Mass Spectrom*. 2015;29:1749-1756.
77. Gómez-Ríos GA, Liu C, Tascon M, et al. Open port probe sampling interface for the direct coupling of biocompatible solid-phase microextraction to atmospheric pressure ionization mass spectrometry. *Anal Chem*. 2018;89:3805-3809.

How to cite this article: Campbell JL, Kafle A, Bowman Z, Blanc JCYL, Liu C, Hopkins WS. Separating chiral isomers of amphetamine and methamphetamine using chemical derivatization and differential mobility spectrometry. *Anal Sci Adv*. 2020;1:233-244.

<https://doi.org/10.1002/ansa.20200066>